

Simple modeling of the thermal history of d.c plasma sprayed agglomerated nanosized zirconia particles

F. Ben Ettouil¹, O. Mazhorova², B. Pateyron¹, Hélène Ageorges¹, M. El Ganaoui¹, P. Fauchais¹

¹ University of Limoges, SPCT, Limoges, France

² Keldysh Institute of Applied Mathematics, Moscow, Russia

Abstract: In this work, are presented the results of a model coupling both dynamic and thermal histories of a single zirconia particle injected into a d.c plasma jet. The model developed calculates the heat transfer and phase changes within the particle along its trajectory. It is based on the Stefan problem with an explicit determination of the position of the interface solid/liquid. The evaporation is described according to the approach “Back pressure” The model is adapted to the calculation of thermal and dynamic behaviors of agglomerated particles

Keywords: fast modelling, d.c plasma spray, agglomerated zirconia particle, thermal history

Nomenclature:

a: thermal accommodation coefficient (= 0.8)
 Bi: Biot number (-)
 c_p : specific heat at constant pressure ($\text{J.kg}^{-1}.\text{K}^{-1}$)
 c_v : specific heat at constant volume ($\text{J.kg}^{-1}.\text{K}^{-1}$)
 C_D : drag coefficient (-)
 d_p : particle diameter (m)
 f', f'' : correction factors of drag coefficient (-)
 f_0, f_1, f_2 : correction factor of Nusselt number (-)
 h : heat transfer coefficient ($\text{W.m}^{-2}.\text{K}^{-1}$)
 $Kn = 1 / d_p$: Knudsen number (-)
 l : mean free path (m)
 L_{sl} : melting latent heat (J.kg^{-1})
 L_{lv} : boiling latent heat (J.kg^{-1})
 m : mass (kg)
 M : molar mass (kg.mole^{-1})
 $Ma = \frac{\text{gas velocity}}{\text{sound velocity}}$: Mach number (-)
 $Nu = hd / \mu$: Nusselt number (-)
 p : pressure (Pa)
 p_s : saturation pressure (Pa)
 $Pe = d.v. \rho.c_p / \kappa$: Peclet number (-)
 $Pr = \mu.c_p / \kappa$: Prandtl number (-)
 r : particle radius (m)
 R : perfect gas constant = $8.314 \text{ (J.mol}^{-1}.\text{K}^{-1})$
 $Re = \rho(v_\infty - v_p).d_p / \mu$: Reynolds number relatively to the particle (-)
 T : temperature (K)
 T_a : room temperature (K)
 u : velocity of vapor (m.s^{-1})
 v : velocity (m.s^{-1})
 $v_T = \sqrt{\frac{8.R.T_s}{\pi.M}}$: mean molecular speed (m.s^{-1})
 ϑ_{sl} : Velocity of the melting front (m.s^{-1})
 ϑ_{lv} : Velocity of the vaporization front (m.s^{-1})
 α : porosity (-)
 β : dimensionless vapor velocity (-)
 $\gamma = c_p / c_v$: Ratio of heat capacities (-)

κ : thermal conductivity ($\text{W.m}^{-1}.\text{K}^{-1}$)
 μ : molecular viscosity (Pa.s)
 ρ : mass density (kg.m^{-3})
 σ : Stefan-Boltzmann constant = $5.67 \cdot 10^{-8} \text{ (W.m}^{-2}.\text{K}^{-4})$
 Indices:
 eb: ebullition
 l: liquid
 p: particle
 sat: saturation
 s: solid
 v: vapor
 ∞ : plasma far from particle

1. Introduction

The plasma spraying of nanosized agglomerated particles aims at building partially nanostructured coatings [1]. Particles must be only partially melted to keep their nanostructured core. So the control of the melting within particles is the key point to achieve successful plasma sprayed partially nanostructured coatings.

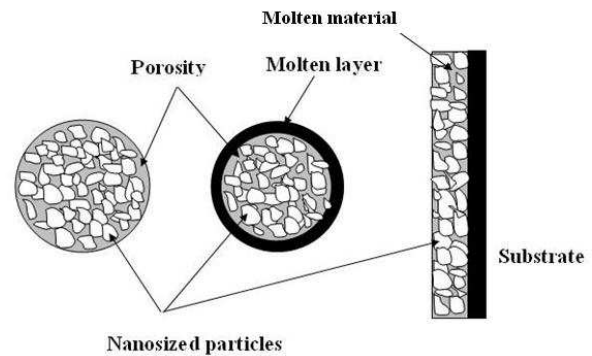


Fig. 1 Mechanism of nanostructured coating building

Such coating are characterized by their increased diffusivity and hardness, reduced density and elastic modulus, improved ductility and lower thermal conductivity [2, 3]

This paper presents the fast modeling of the thermal history of a single nanosized agglomerated zirconia particle d.c plasma sprayed. After the brief recall of the 2D parabolic model of the plasma jet, are described the modeling of the particle trajectory and heating including the propagation of melting or solidification or vaporization front and finally results obtained with the porous zirconia particles.

2. Modeling

2.1. Plasma jet modeling

“Jets&Poudres” software [4], dealing with 2D parabolic flow, was used to model the plasma jet, assumed to be stationary. Although this model neglects the interaction between carrier gas flow and the plasma flow, results are in good agreement with those obtained with a 3D more sophisticated code, taking this interaction into account [5]. Figure 2 presents the temperature field of the d.c plasma jet simulated with working conditions summarized in table 1 (which will be used in the following), and the trajectory of a single zirconia particle 30μm in diameter.

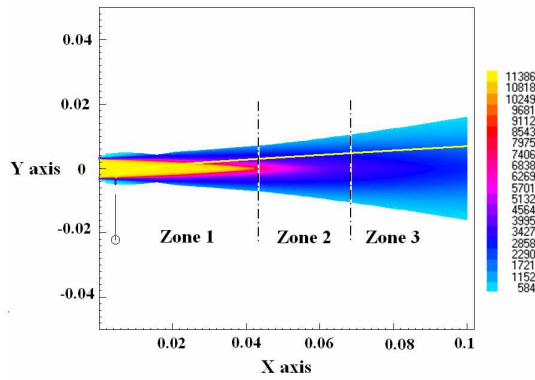


Fig. 2 Temperature fields and trajectory of a single zirconia particle ($d_p = 30\mu\text{m}$) in the plasma jet.

Table 1. Torch working conditions

Plasma gas	H ₂ -Ar 75% vol
Nozzle internal diameter	7 mm
Plasma gas flow rate	60 L/min
Spray distance	100 mm
Surrounding atmosphere	Air
Electric power	32 kW
Thermal efficiency	57 %
Effective thermal power	18.24 kw

2.2 Particle Dynamic Modeling

The single particle trajectory is calculated from the force balance exerted on it. Most numerical works for d.c plasma jet take into account only the drag forces [6]. The momentum equation is written as follows:

$$m_p \cdot \frac{dv}{dt} = \frac{1}{2} C_D \pi \frac{d_p}{4} \rho_\infty |v_\infty - v_p| (v_\infty - v_p)$$

Corrective factors to the drag coefficient are introduced to take into account the drastic gradients of temperature and gas properties within the thermal boundary layer surrounding the particle, as well as the Knudsen effect. It follows:

$$C_D = \frac{24}{\text{Re}} (1 + 0.11 \cdot \text{Re}^{0.81}) f f''$$

where f' is the corrective coefficient suggested by Lee [7] to take into account the temperature gradient within the boundary layer and f'' is that corresponding to the Knudsen effect [8] which is not negligible for particles with $d_p < 20 \mu\text{m}$.

2.3 Particle heating Modeling

In the plasma jet conditions, the coefficient of heat transfer h is written as follows:

$$h = \frac{Nu \cdot \bar{\kappa}}{d_p}$$

Where $\bar{\kappa}$ is the integrated thermal conductivity as proposed by Bourdin et al [9]

$$\bar{\kappa}(T) = \frac{1}{T - T_a} \int_{T_a}^T \kappa(\theta) d\theta$$

The thermal conductivity of a nanosized agglomerated particle is calculated as function of its porosity α

$$\kappa_{eff} = \kappa_s (1 - \alpha) \quad (\kappa_s = 1.66 \text{ Wm}^{-1} \text{K}^{-1})$$

As for the drag coefficient, and taking into account the variations of plasma properties within the boundary layer, corrective coefficients are introduced in the modified Nusselt number:

$$Nu = (2 + 0.6 \text{Re}_p^{0.5} \text{Pr}_p^{0.33}) f_0 f_1 f_2 \quad (8)$$

f_0 , f_1 and f_2 being respectively the corrective factors related to the temperature gradient within the boundary layer, the Knudsen effect and the vapor buffer around the particles [8, 10, and 11]

The progress of the evaporation front is deduced from the equation of mass conservation:

$$\rho_l v_{lv} = \rho_v (v_{lv} - u)$$

To uncouple the calculation of the evaporation of the particle and its dynamic, the result of J. C. Knight [12] has been used. He has treated the Knudsen layer as a gas dynamic discontinuity: the approximate jump conditions were derived and, particularly, gave the mass fraction of flow leaving the Knudsen layer, for which a jump condition was written as follows:

$$\frac{T}{T_s} = \left[\sqrt{1 + \pi \left(\frac{\gamma - 1}{\gamma + 1} \frac{\beta}{2} \right)} - \sqrt{\pi} \frac{\gamma - 1}{\gamma + 1} \frac{\beta}{2} \right]^2$$

$$\frac{\rho}{\rho_s} = \sqrt{\frac{T}{T_s}} \left[\left(\beta^2 + \frac{1}{2} \right) e^{m^e} \text{erfc}(\beta) - \frac{\beta}{\sqrt{\pi}} \right]$$

$$+ \frac{1}{2} \frac{T}{T_s} \left[1 - \sqrt{\pi} \beta e^{m^e} \text{erfc}(\beta) \right]$$

β being the dimensionless velocity of vapor as proposed by Knight [13] and Ma the mach number:

$$Ma = \frac{u}{\sqrt{\frac{\gamma RT}{M}}} = \beta \cdot \sqrt{\frac{2}{\gamma}}$$

Of course the particle trajectory calculation takes into account, at time t_{i+1} , its mass loss by evaporation calculated at time t_i . W_{fr} defined as the mass fraction leaving the particle through the Knudsen layer (the

adjacent field to the particle) is described by the continuous averaged equations:

$$W_{fr} = \frac{\rho_v u}{\rho_{sat} \sqrt{RT/2\pi M}}$$

Taking into account the approximation $\rho_v \ll \rho_l$ and the equation of state of perfect gases $p_{sat} = \rho_{sat} (R/M) T$, the evaporation front velocity can be written as follows:

$$\vartheta_{lv} = -\frac{W_{fr} \rho_{sat} \sqrt{RT/M}}{\rho_l} = -\frac{1}{\sqrt{2\pi}} \frac{W_{fr}}{\rho_l} \frac{p_{sat}}{\sqrt{RT/M}}$$

The saturated vapor pressure p_{sat} at the temperature T is given by:

$$p_{sat} = p_{eb} \exp \left[\frac{M \cdot L_{lv}}{RT_{eb}} \left(1 - \frac{T_{eb}}{T} \right) \right]$$

The moving interface is treated within an adaptive grid in which the positions of different phase change fronts are fixed. The transformation of co-ordinates thus depends only on interface velocities [13]. An implicit scheme of finished differences is written. The dynamic and thermal simulations of a single particle are thus carried out by minimizing the time costs of calculations.

3. Results

Figure 3 presents the axial evolution of the melting front within three agglomerated zirconia particles of different sizes with $\kappa_{eff} = 1.16 \text{ W.m}^{-1}.\text{K}^{-1}$. It allows evaluating the size of the nanostructured core, preserved at the end of the heat treatment of zirconia particles. The particle $40 \mu\text{m}$ in diameter is totally melted when within particles of 50 and $60 \mu\text{m}$ remain nanostructured solid core respectively of 27 and $56 \mu\text{m}$ corresponding to 54 and 71 % of their initial diameter. This result shows that there is a lower limit to the particle size over which nanostructured solid core can be obtained.

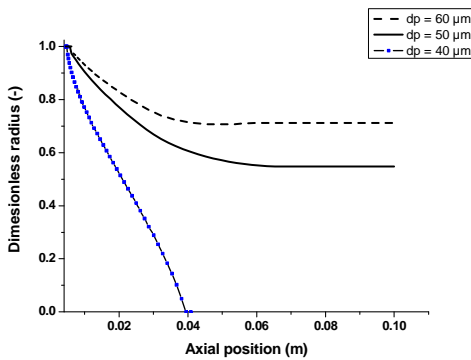


Fig. 3 Axial evolution of the melting front in agglomerated zirconia particles.

In figure 4 is presented the axial evolution of the melting front in an agglomerated zirconia particle $60 \mu\text{m}$ in diameter but injected with three different initial velocities. It is obvious that the melting state is controlled by the residence time within the plasma jet core, ie the hottest zone of the plasma jet. With an initial velocity of 14 m.s^{-1} the particle stays in this zone until its end and

receives an important thermal energy flux, thus its melting degree is more important than that of the particle injected at 17 or 20 m.s^{-1} which cross the plasma jet core with shorter residence times. (15)

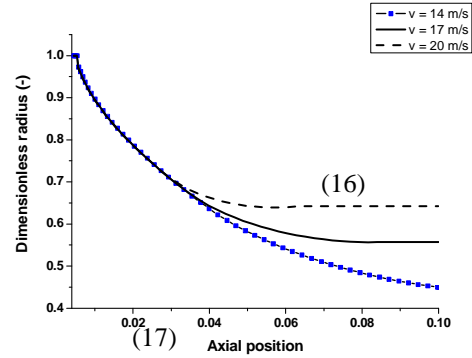


Figure 4 Axial evolution of the melting front in agglomerated zirconia particle ($dp = 60 \mu\text{m}$, $\kappa_{eff} = 1.16 \text{ W.m}^{-1}.\text{K}^{-1}$).

Figure 5 shows the evolution of the melting front as a function of the axial position for three zirconia particles both $60 \mu\text{m}$ in diameter but with different porosities. The size of the nanostructured core preserved is inversely proportional to the porosity.

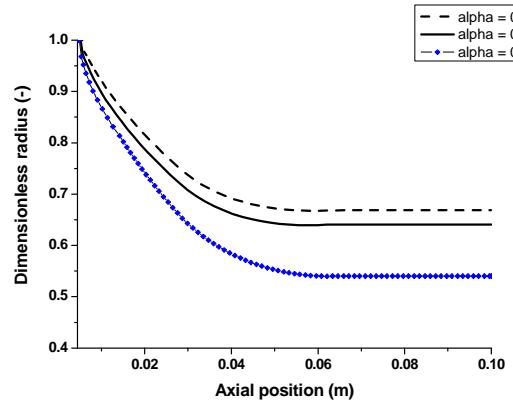


Figure 5 Axial evolution of the melting front in agglomerated zirconia particle ($dp = 60 \mu\text{m}$). ($\alpha = 0.1 \kappa_{eff} = 1.49$; $\alpha = 0.3 \kappa_{eff} = 1.16$; $\alpha = 0.5 \kappa_{eff} = 0.83$)

Particle diameter variation is controlled by both its vaporization and withdrawal due to the porosity loss. Figure 6 illustrates the evolution of the size of three zirconia particles all $60 \mu\text{m}$ in diameter but with different porosities. It is clear that the particle with the lowest porosity ($\alpha = 10\%$) loses only 2.87 % of its initial diameter, however, this loss is increased to 15 % with 50 % porous particle. The knowledge of this size variation is important for the simulation and control of flatter of the partially melted particles on the substrate.

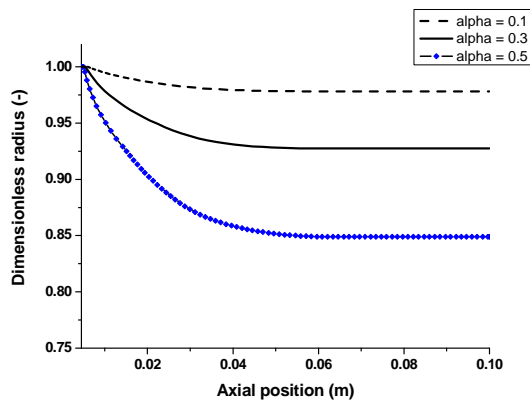


Figure 6 Axial evolution of particle size in agglomerated zirconia particle ($d_p = 60 \mu\text{m}$).

5. Conclusions

A model dealing with thermal and dynamic behaviours of particles within stationary d.c. plasma jets has been developed. Phase changes are taken into account by a finite difference scheme and simultaneous moving boundary layers between them. This model presents the advantage of a drastic low cost of calculation time (a few second). It was applied to the study of the thermal history of d.c plasma sprayed agglomerated nanosized zirconia particles, by taking into account the influence of the particle porosity (or thermal properties) and the particle size variation due to the porosity loss and evaporation. This model can be considered as a tool for the optimization of particle injection conditions and diameters that promote an unmelted agglomerated core keeping its initial nanostructure.

References

- [1] R. S. Lima, A. Kucuk and C. Berndt. "Bimodal Distribution of Mechanical Properties on Plasma Sprayed Nanostructured Partially Stabilized Zirconia", *Mat. Sci. Eng.* **A327**, p 224-232 (2002)
- [2] M.Gell, Application opportunities for nanostructured materials and coatings, *Mat. Sci. Eng.* **A204**, p 246-251 (1995)
- [3] T. Grosdidier, G. Ji and N. Bozzolo. "Hardness, thermal stability and yttrium distribution in nanostructured deposits obtained by thermal spraying from milled - YO reinforced - or atomized FeAl powders, *Intermetallics*, **14** (7), p 715-721 (2002)
- [4] <http://www.unilim.fr/spcts/>
- [5] G. Delluc, H. Ageorges, B. Pateyron, P. Fauchais, Fast Modeling of Plasma Jet and Particle Behaviors in spray conditions, *High Temp. Mat. Processes*, **9**, p211-226, (2005)
- [6] E. Pfender, Particle Behaviour in Thermal Plasma, *Plasma Chem. And Plasma Proc.* **9** (1) p 167S-194S (1989)
- [7] Y.C. Lee, C. Hsu, E. Pfender, "Modelling of particle injection into a D.C Plasma Jet" 5th International Symposium on Plasma Chemistry, Edinburgh, Scotland, 2, p 795-801, (1981)
- [8] X.Chen, Heat and Momentum Transfer between thermal plasma and suspended Particles for Different Knudsen Numbers. *Thin Solid Films*, 345, p 140-145,

(1999)

- [9] E. Bourdin, P. Fauchais, M. Boulos, Transient heat conduction under plasma condition. *Int. J. Heat Mass Transfer* **26** (4), p. 582-652, (1983)
- [10] Y.P. Wan, V. Prasad, G-X Wang, S. Sampath, J.R. Fincke, Model and Powder Particle Heating, Melting, Resolidification, and Evaporation in Plasma Spraying Processes. *J. Heat Transfer ASME*, **121**, p.691-699. (1999)
- [11] X. Chen, Y.P. Chyou., Y.C. Lee, E. Pfender, Heat-transfer to a particle under plasma Conditions with vapor contamination from the particle. *Plasma Chem. Plasma Process.* **5**, p 119-141, (1985)
- [12] C. J. Knight, Theoretical modelling of rapid surface vaporization with back pressure, *AIAA journal*, **17** (5), p 519-523, (1979)
- [13] H. Hu, S. A Argyropoulos, Mathematical modelling of solidification and melting: a review *Modelling Simul. Mater. Sci. Eng.* **4**, p 371-396, (1996)